General Disclaimer

One or more of the Following Statements may affect this Document

- This document has been reproduced from the best copy furnished by the organizational source. It is being released in the interest of making available as much information as possible.

- This document may contain data, which exceeds the sheet parameters. It was furnished in this condition by the organizational source and is the best copy available.

- This document may contain tone-on-tone or color graphs, charts and/or pictures, which have been reproduced in black and white.

- This document is paginated as submitted by the original source.

- Portions of this document are not fully legible due to the historical nature of some of the material. However, it is the best reproduction available from the original submission.

X-921-75-300

PREPRINT

NASA TM X- 71028

POWER SPECTRA OF GEOID UNDULATIONS

RICHARD D. BROWN

NOVEMBER 1975

GODDARD SPACE FLIGHT CENTER
GREENBELT, MARYLAND

ABSTRACT

POWER SPECTRA OF GEOID UNDULATIONS

Data from spacecraft altimeters are expected to contribute to an improved determination of the marine geoid. The geoid is typically described in terms of undulations, i.e., the distance between the geoid and a reference surface, and these undulations may be recovered from altitude data and knowledge of the spacecraft orbit. To better define altimeter system design requirements for geoid recovery, amplitudes of geoid undulations at short wavelengths are examined. Models of detailed geoids in selected areas around the earth, developed from a combination of satellite derived spherical harmonics and 1^{o}-by-1^{o} area mean free-air gravity anomalies, are subjected to a spectral analysis. The resulting undulation power spectra are compared to existing estimates for the magnitude of geoid undulations at short wavelengths. The undulation spectra are found to be consistent with Kaula's rule of thumb, following an inverse third power relationship with spatial frequency for wavelengths at least as small as 300 km. The requirements imposed by this relationship on altimeter accuracy, data rate, and horizontal resolution to meet the goal of a detailed geoid description are discussed.

CONTENTS

POWER SPECTRA OF GEOID UNDULATIONS FOR THE NORTH ATLANTIC

INTRODUCTION

Data from spacecraft altimeters are expected to contribute to an improved determination of the size and shape of the marine geoid. If the orbit of the spacecraft is known, then altitude data provides a direct estimate of the geocentric radius to the geoid (References 1, 2). Even assuming realistic uncertainties in knowledge of the orbit and geopotential parameters, it is theoretically feasible to recover geoid information in a bootstrap process (References 3, 4, 5, 6).

The shape of the geoid is described in terms of geoid undulation, the normal distance between the geoid surface and some reference surface (Reference 7). The resolution with which this surface can be defined by altimeter measurement is dependent on altimeter design and operation. Three factors related to altimeter hardware and data processing impose practical limits on the detection of small geoid features. First, the geoid undulation must be of sufficient amplitude to be detected by the altimeter; i.e., the measurement error of the altimeter must be less than the geoid undulation amplitude. Second, referring to Figure 1, the effective illuminated surface area (the area illuminated when the detected wavefront intersects the surface) must be smaller than the wavelength of the undulation to be measured. Finally, the sampling rate of the altimeter, $1/\tau_s$ (sec^{-1}), must be such that two measurements can be made within one wavelength of the undulation to be measured (Reference 8). For example, the feature depicted at the far left of Figure 1 probably would not be resolved by the altimeter due to effective illuminated area constraints as well as data rate constraints.

To evaluate these factors in a simulated operational environment, the best available geoid models, i.e., detailed gravimetric geoids developed by Vincent, et al (Reference 9 10), were chosen for undulation power spectra analysis. Several authors, notably Kaula (References 11, 12) and Rapp (References 13, 14) have analyzed the power

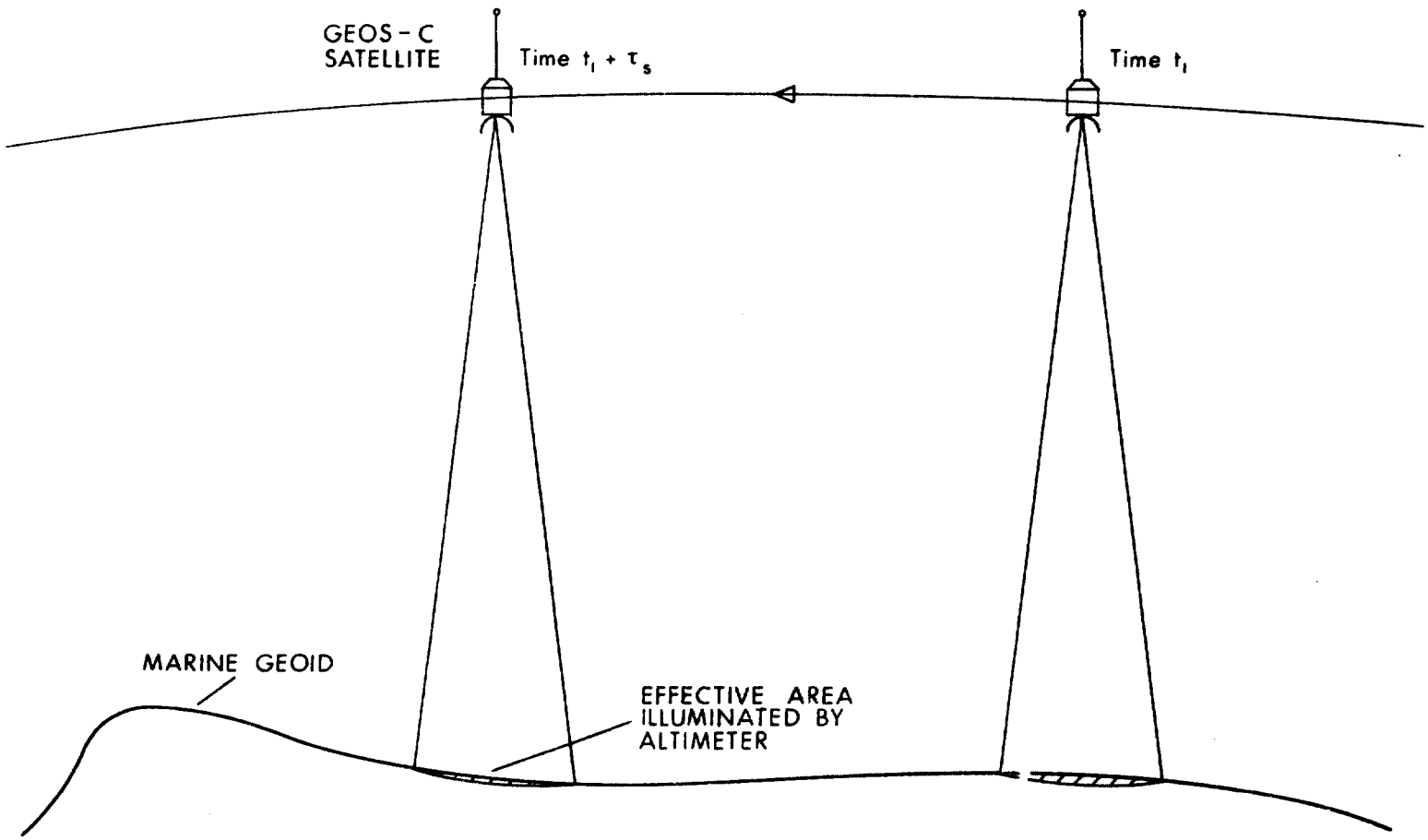

Figure 1. ALTIMETER MEASUREMENT GEOMETRY

spectra of gravity anomalies and the gravity potential from observed and modeled gravity data. These gravity spectra imply a certain shape for the undulation power spectrum on a world-wide basis (Reference 15). However, a smaller quantity of less detailed gravity data was used in these analyses than is incorporated in the geoid models selected for this analysis.

A capability for computation of autocovariance of geoid heights in two dimensions which eliminates the need for averaging and fitting of curves to one-dimensional profiles, was used in the spectral analysis of nine local geoid areas. These spectra are compared to the spectra of related geophysical parameters, and appropriate conclusions are drawn for modeling the spectrum and for altimeter design and operation.

ANALYSIS

Detailed Geoid Model

The geographical areas chosen for evaluation cover about one-fourth of the globe. These areas, depicted in Figure 2, are described as the North-East Pacific, Canada, United States, South America, North Atlantic, Europe, Eurasis, India, and Australia. For these areas geoid heights were available at 1^{o} intervals. These heights were generated by combining 1^{o}-by-1^{o} area mean free-air gravity anomalies with gravity anomalies calculated from the spherical harmonic coefficients of the SAO'69 geopotential model and using Stokes' formula following the method used by Vincent, et al (Reference 9). The geoid undulation N is expressed by Stokes' formula as

$$N(\phi,\lambda) = \frac{R}{4\pi\gamma} \int_{\lambda'=0}^{2\pi} \int_{\phi'=-\pi/2}^{\pi/2} \Delta g(\phi',\lambda')\, S(\psi)\, \cos\phi'\, d\phi'\, d\lambda' \quad \text{(meters)} \qquad (1)$$

where ϕ, λ are the latitude and longitude, respectively, of the computational point in radians

ϕ', λ' are the latitude and longitude, respectively, of the variable integration point in radians

R is mean earth radius (m)

γ is mean gravitational acceleration at the earth's surface in m/sec^2

$\Delta g(\phi', \lambda')$ is the mean free-air gravity anomaly at (ϕ', λ') in m/sec^2

$S(\psi)$ is Stokes' function, $S(\psi) = \csc\left(\frac{\psi}{2}\right) - 6 \sin\left(\frac{\psi}{2}\right) + 1 - 5 \cos\psi - 3 \cos\psi \ln\left[\sin\left(\frac{\psi}{2}\right) + \sin^2\left(\frac{\psi}{2}\right)\right]$

ψ is the great circle central angle between (ϕ, λ) and (ϕ', λ') in radians

This integral is carried out over the entire spherical surface defined by the mean radius R. Because of the behavior of Stokes' function, however, the effect of gravity anomalies in regions distant from the evaluation point (ϕ, λ) is negligible. Accordingly, the region of integration is divided in equation (1) into two areas; a local area A_1 surrounding (ϕ, λ) and the remainder of the sphere, denoted A_2. The anomalous gravity field in each region is also divided into two parts; a gravity anomaly Δg_s corresponding to low order and degree spherical harmonies derived from satellite tracking data, and a gravity anomaly Δg_2 defined by

$$\Delta g\ (\phi, \lambda) = \Delta g_s\ (\phi, \lambda) + \Delta g_2\ (\phi, \lambda) \tag{2}$$

where Δg is the mean free-air gravity anomaly at (ϕ, λ).

Thus equation (1) can be rewritten as:

$$N(\phi, \lambda) = N_1(\phi, \lambda) + N_2(\phi, \lambda) + N_3(\phi, \lambda) \tag{3}$$

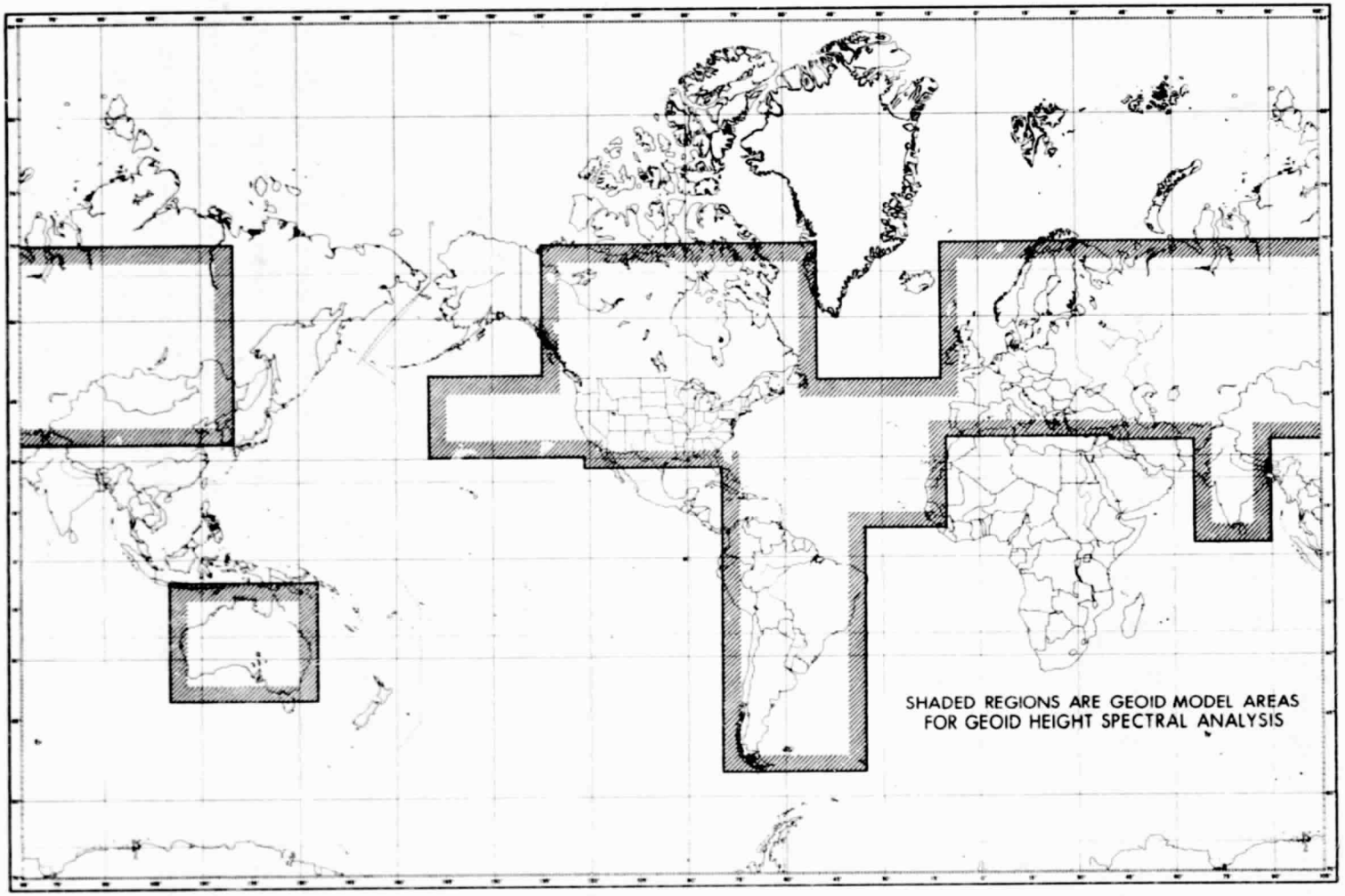

Figure 2. AREAS REPRESENTED BY DETAILED GEOID MODELS

where

$$N_1 = \frac{R}{4\pi\gamma} \int_0^{2\pi} \int_{-\pi/2}^{\pi/2} \Delta g_s\,(\phi', \lambda')\, S(\psi)\, \cos\phi'\, d\phi'\, d\lambda'$$

$$N_2 = \frac{R}{4\pi\gamma} \int_{A_1} \int \Delta g_2\,(\phi', \lambda')\, S(\psi)\, \cos\phi'\, d\phi'\, d\lambda' \qquad (4)$$

$$N_3 = \frac{R}{4\pi\gamma} \int_{A_2} \int \Delta g_2\,(\phi', \lambda')\, S(\psi)\, \cos\phi'\, d\phi'\, d\lambda'$$

The term N_1 can be calculated by numerical integration or by iterative inverse interpolation (Reference 9). N_2 is evaluated by a summation approximation over a 20^o-by-20^o square area A_1 centered at the evaluation point with data at a grid interval of 1^o-by-1^o (mean free-air gravity anomalies are available for 1^o-by-1^o square areas). Since the magnitude of the Stokes' function is known to be much smaller in area A_2 than in A_1, N_3 is taken to be negligible.

The accuracy of this calculation of N is estimated (Reference 9) to be ±2m on land and in coastal areas and ± 7m in areas where surface gravity data is less dense. Figure 3 shows a contour map for the North Atlantic area as a typical local geoid model.

Generation of Power Spectra

In general, three steps are involved in the generation of powe. spectra. These are the calculation of covariance functions, the application of a discrete cosine series transform to the covariance functions to generate "raw" power spectral density values, and the smoothing of these "raw" values to compensate for the effects of frequency analysis on a record of finite length. The following text treats these three steps in more detail.

Blackman and Tukey (Reference 16) give for autocovariance in one dimension at r arc degrees

$$C_r = \frac{1}{n-r} \sum_{q=1}^{n-r} N_q \cdot N_{q+r} \quad , \; r = 0, 1, 2, \ldots\ldots m, \text{ in (meters)}^2 \qquad (5)$$

where m is the maximum number of lags or the largest correlation distance in terms of 1 arc degree intervals to be examined

n is the total number of data points spaced at 1 arc degree intervals

N_q is the q^{th} geoid undulation, adjusted to zero mean on the set of n values

For a two-dimensional array of data, such as in the detailed geoid models, the auto-covariance calculation is much more complicated, involving a sum of products of the undulation at a particular point p and the undulation at a point between r and r + 1 arc degrees distance from p. This sum is carried out over all points p and over all points within the (r, r + 1) distance criteria from each point p, with the proviso that no particular undulation product pair be represented in the summation more than once. This sum must be normalized by the number of undulation pair products included in the sum. The actual calculation is carried out in a computer program and involves too many logical statements and tests to present here. However, the calculation may be represented in a pseudo-mathematical form by

$$C_r = \frac{1}{\rho \cdot c \cdot P(r)} \sum_{q=1}^{\rho} \sum_{s=1}^{c} \sum_{q' \, s'} N_{q,s} \; N_{q's'} \qquad (6)$$

where ρ is the number of rows in the data array

c is the number of columns in the data array

q', s' are the indices of any data point lying between r and r + 1 arc degrees distance from the point q, s

$\sum_{q', s'}$ indicates a summation over all points q' s' such that no duplication of products $N_{q,s} \; N_{q',s'}$ occurs in the total summation of equation (6).

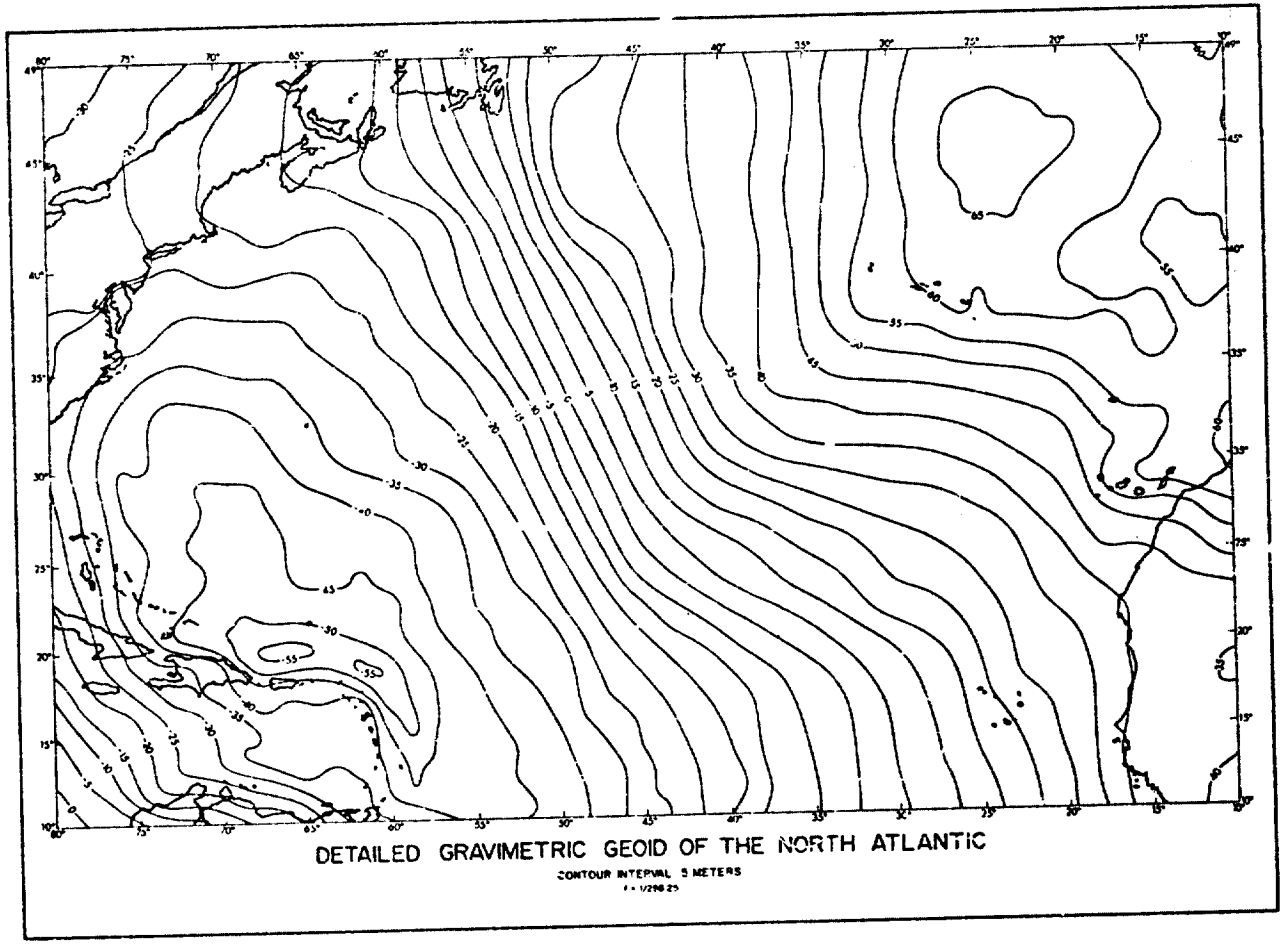

Figure 3. DETAILED GRAVIMETRIC GEOID OF THE NORTH ATLANTIC

$P(r)$ is the number of data points q', s' included in the summation $\sum_{q' s'}$ for a given value of r.

This evaluation of the autocovariance is based on the assumption that the autocovariance of geoid undulations is isotropic.

Next a discrete finite cosine series transform is applied to the autocovariance values to obtain a 'raw' PSD function value,

$$V_r = 2 \left[C_o + 2 \sum_{q=1}^{m-1} C_q \cos \frac{qr\pi}{m} + C_m \cos r\pi \right] m^2/\text{cycle/arc degree} \quad (7)$$

This raw estimate must be smoothed to compensate for discontinuities inherent in the digital discrete cosine transform process. The process known as "hamming" (Reference 16) is used as follows, resulting in the smoothed power spectrum estimate,

$$\begin{aligned} \tilde{V}_o &= .54\, V_o + .46\, V_1 \\ \tilde{V}_r &= .23\, V_{r-1} + .54\, V_r + .23\, V_{r+1} \qquad r = 1, 2, \ldots, m-1 \\ \tilde{V}_m &= .46\, V_{m-1} + .54\, V_m \end{aligned} \quad (8)$$

Referring to equation (7) it is clear that a large maximum lag distance (large m), subject always to

$$m < M$$

where M = the smaller of ρ or c,

will result in a large number of PSD estimates within the desired frequency band and therefore yield good frequency resolution. But PSD estimate accuracy decreases as the index r approaches m. The error E in the smoothed power spectrum (PS) is given (Reference 17) as a function of m and M as

$$E = \sqrt{m/M} \quad (9)$$

The use of large m values may also cause instability in the calculation of PSD values as r approaches m. Instability in the PS plot manifests itself as periodic fluctuations in the PS as r approaches m. That is, the instability occurs at frequencies near the high frequency limit, which is the folding frequency

$$f_c = \frac{1}{2h} \quad \text{(cycle/deg.)} \tag{10}$$

where h is the interval between data points, i.e., 1 arc degree.

Exercising the tradeoff between resolution and accuracy or stability is largely a matter of cut-and-try in the choice of maximum lag value m, although Blackman and Tukey (Reference 16) recommend

$$m \leq .10\,M \tag{11}$$

After several PS plots for local geoids were generated, aliasing of the folding frequency was detected in the spectra. This effect is one of the pitfalls of sampling data at a regular interval and is manifest as artificial peaks in the power spectrum at rational fractions of the folding frequency,

i.e., $\frac{f_c}{2}$, $\frac{f_c}{3}$, $\frac{f_c}{4}$, etc.

To remove this alias (to first order) power spectral density values were calculated, by the above method, using data whose power spectrum is known and which is similar to the geoid P.S. Aliased peaks in this calculated spectrum were easily identified and separated from the true spectrum. They were then normalized and subtracted from the calculated spectra for geoid heights.

Kaula's Rule of Thumb

This rule, derived from analysis of gravity anomalies (Reference 12), estimates the root-mean square value of the spherical harmonic geopotential coefficient of degree n from

$$\sigma_n \left\{ \bar{C}_{nm}, \bar{S}_{nm} \right\} = \frac{\pm 10^{-5}}{n^2} \tag{12}$$

By expressing geoid undulation in spherical harmonics, the degree variance of geoid heights may be written (Reference 14) as

$$\sigma_n^2 \left\{ N \right\} = \frac{\mu}{\gamma} (2n+1) \sigma_n^2 \left\{ \bar{C}_{nm}, \bar{S}_{nm} \right\} \quad (\text{meter})^2 \tag{13}$$

where μ is the Earth's gravitational constant and γ is the average acceleration of gravity at the Earth's surface.

By substituting equation (12) into equation (13), it is seen that Kaula's rule-of-thumb implies

$$\sigma_n^2 \left\{ N \right\} = \frac{\mu \times 10^{-10}}{\gamma} \left(\frac{2n+1}{n^4} \right) \quad (\text{meter})^2 \tag{14}$$

The degree variance of N may be interpreted as the average amplitude squared of geoid undulation at a particular frequency, f_n,

where $$f_n = \frac{n}{360 \text{ arc degrees}} \tag{15}$$

it represents the value of the power spectra of geoid undulations at a particular frequency. If a continuum of frequencies is assumed than from equations 14 and 15 it is expected that the power spectra of geoid undulations V(f) would be approximately proportional to f^{-3},

$$V(f) = \frac{K}{f^3} \tag{16}$$

at high frequencies, if Kaula's rule-of-thumb remains valid.

MODELING THE SPECTRA

Figure 4 shows a pair of typical PSD plots, one for the area defined by the continental United States and one for the Northeast Pacific area. Both plots show good agreement with the f^{-3} rule implied by Kaula's rule-of-thumb. These plots also point up the general similarity between PSD plots of land and ocean geoid areas, a similarity that was observed for all nine geoid areas. This similarity is not expected to hold for frequencies much higher than 0.5 cycles per arc degree due to the high amplitude undulations at short wavelengths expected in mountainous regions. The small peaks evident at the high frequency end of these plots are probably due to imperfect correction of the spectra for aliasing of the folding frequency. These plots were truncated at 0.4 cycles per arc degree because of aliasing of higher frequency undulations at frequencies between 0.4 and 0.5 cycles per arc degree.

Figure 5 shows the consistency of the chosen f^{-3} rule spectra model with all nine PSD plots. The placement of this f^{-3} line for the derived spectra was adjusted to best approximate the PSD values of the two marine geoid areas represented, i.e., the North Atlantic and the Northeast Pacific areas. The chosen model is represented by

$$V = \frac{0.0525}{f^3} \quad m^2/\text{cycles/arc degree for } f \text{ in cycles/arc degree} \qquad (17)$$

TYPICAL GEOID UNDULATION POWER SPECTRA

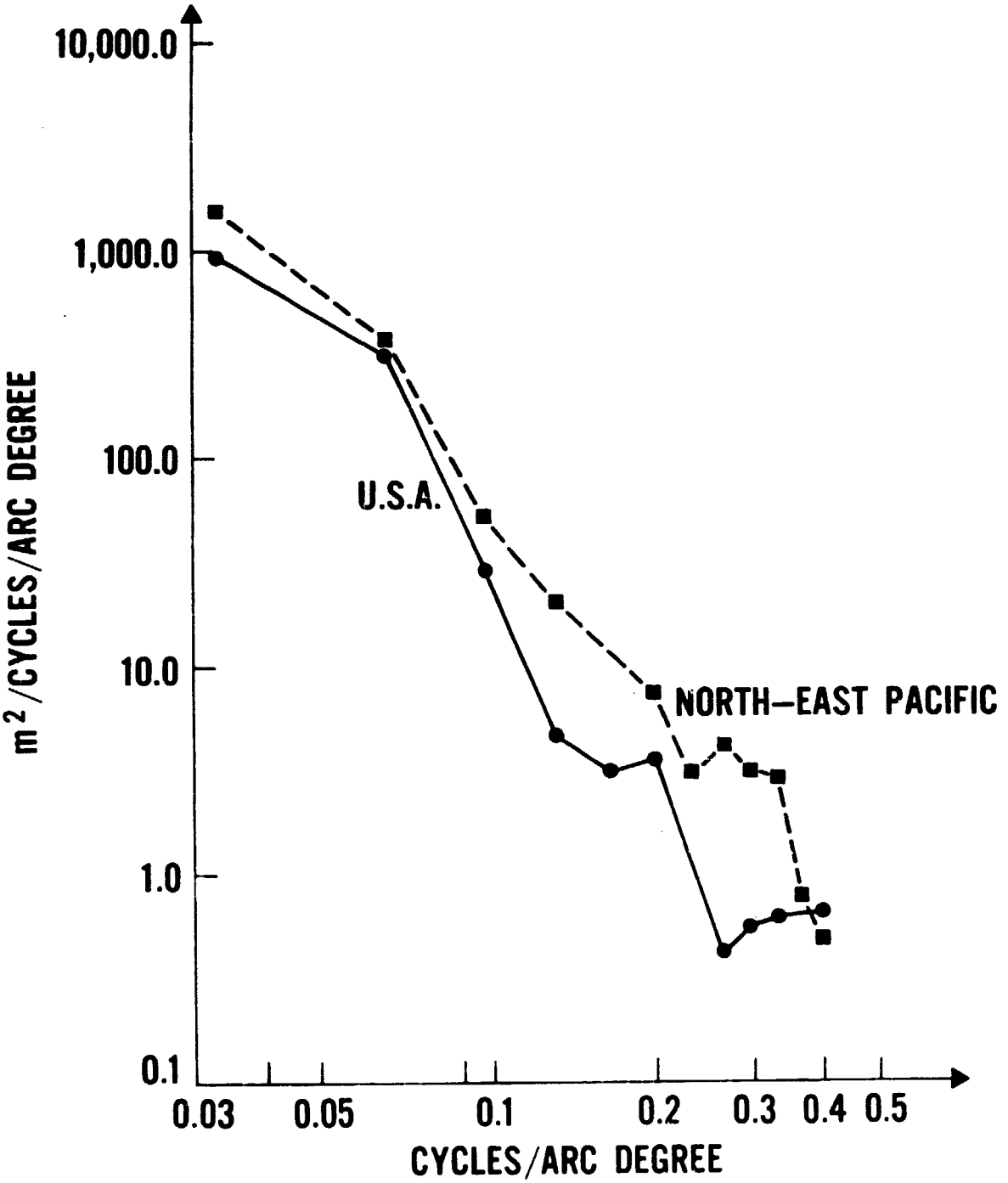

Figure 4

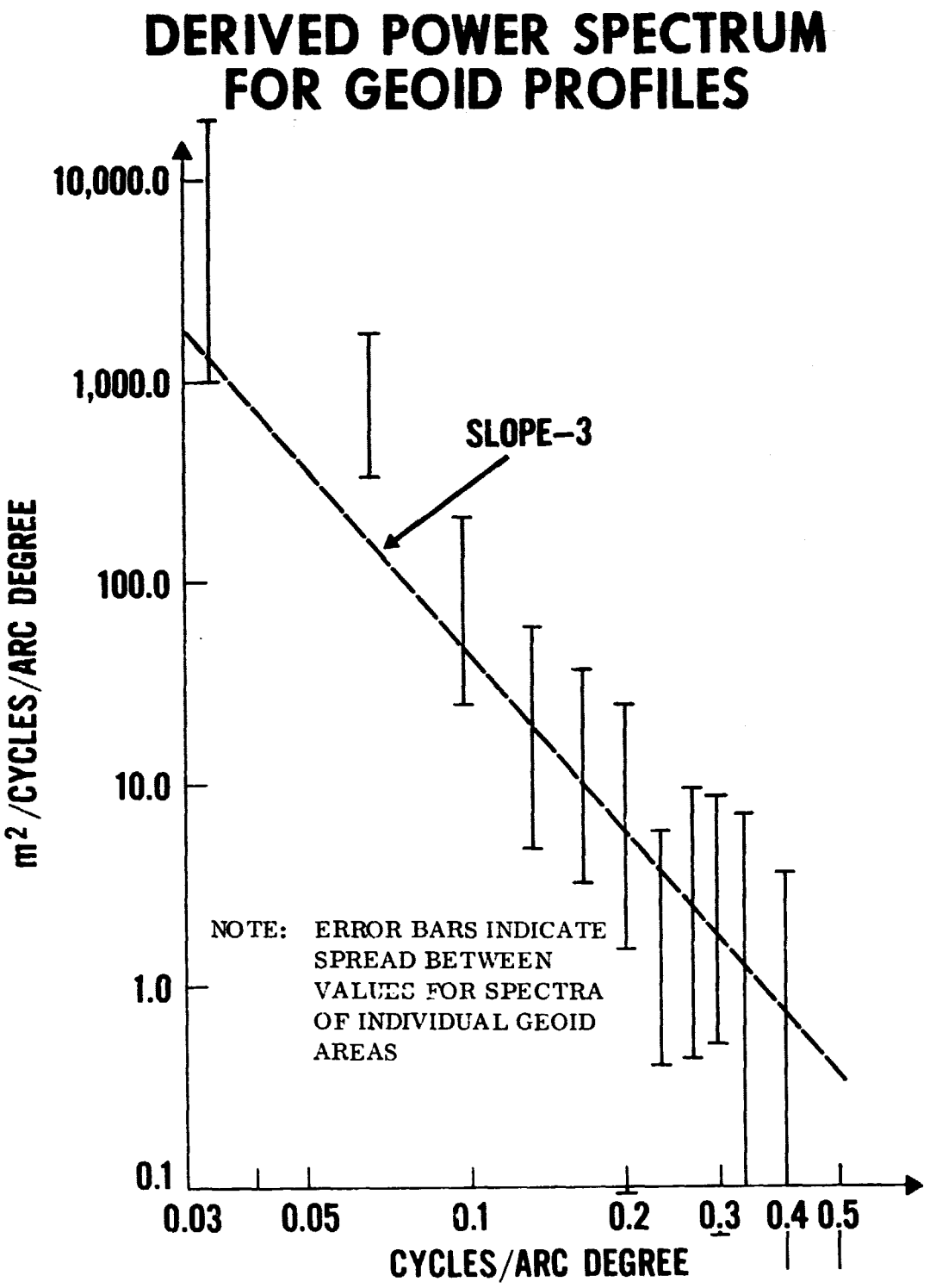
DERIVED POWER SPECTRUM
FOR GEOID PROFILES
10,000.0
1,000.0
100.0
10.0
1.0
0.1
m² /CYCLES/ARC DEGREE
SLOPE–3
NOTE: ERROR BARS INDICATE SPREAD BETWEEN VALUES FOR SPECTRA OF INDIVIDUAL GEOID AREAS
0.03
0.05
0.1
0.2
0.3
0.4
0.5
CYCLES/ARC DEGREE

Figure 5

DISCUSSION OF RESULTS

To assess the effect of the geoid spectra model on altimeter design and operation, assume an altimeter height resolution capability of ± 1m. From Figure 5, a 1m undulation (represented as $1m^2$/cycle/arc degree) is found to correspond to a frequency of 0.374 cycles/arc degree. Since 1 arc degree = 111 km., this frequency represents an undulation wavelength of 296 km. This represents, on average, the short wavelength limit for undulations that can be detected by an altimeter with 1 meter resolution capability. However, actual resolution of this undulation also requires that the diameter of the surface area spot illuminated by the altimeter be much smaller than 296 296 km., and the altimeter sampling rate must be such that at least two measurements be made in this distance. This implies a data rate of at least 2 measurements per minute at a typical satellite ground speed of 8 km./second. The GEOS-C altimeter, which has a planned 1 meter height resolution, should be able to detect and measure 296 km. wavelength undulations in the North Atlantic since its effective illuminated spot diameter is about 12 km. and its sampling rate is at least 10 samples/second (Reference 18).

CONCLUSIONS

The power spectra of geoid undulations for the detailed geoid model are found to be not inconsistent with Kaula's rule-of-thumb for the magnitude of harmonic coefficients of different degree, following an inverse third power law with frequency.

For an altimeter of 1m precision operating over ocean areas, the geoid undulation power spectra imply requirements for at least a 2.0 measurement per minute data rate and a spot size of less than 50 km. diameter in order to resolve undulations of 1m amplitude.

REFERENCES

1. Strange, W. E.; "Marine Geodesy"; EOS, Transactions of the AGU, Volume 52, No. 3; March 1971.

2. Hudson, E. F.; "Determining the Geometric Shape of the Geoid in Ocean-Covered Areas of the World by Satellite Radar Altimeter" (abstract); EOS, Transactions of the AGU, Volume 51, pg. 263; 1970.

3. Greenwood, J. A., et al; "Radar Altimetry from a Spacecraft and its Potential Applications to Geodesy and Oceanography"; NYU School of Engineering and Science, Department of Meteorology and Oceanography; Report on Contract N62306-1589, U. S. Naval Oceanographic Office; May 1967.

4. Lundquist, C. A., Giacaglia, G. E. O., Hebb, K., Mair, S. G.; "Possible Geopotential Improvement from Satellite Altimetry"; SAO Report No. 294; 1970.

5. Young, R. G. E.; "Combining Satellite Altimetry and Surface Gravimetry in Geodetic Determinations"; MIT Measurement Systems Lab., Report RE 37; 1970.

6. Koch, K. R.; "Gravity Anomalies for Ocean Areas from Satellite Altimetry"; Proceedings of the Second Marine Geodesy Symposium, Marine Technology Society; Washington, D. C.; 1970.

7. Heiskanen, W. A. and Moritz, H.; Physical Geodesy; W. H. Freeman & Co.; 1967.

8. Papoulis, A.; "Probability, Random Variables, and Stochastic Processes"; McGraw Hill; 1965.

9. Vincent, S., Strange, W. E., Marsh, J. G.; "A Detailed Gravimetric Geoid from North America to Europe"; NASA GSFC Document X-553-72-94; March 1972.

10. Vincent, S., Strange, W. E., and Marsh, J. G., "A Detailed Gravimetric Geoid of North America, the North Atlantic, Eurasia, and Australia"; NASA GSFC Document X-553-72-331; September 1972.

11. Kaula, W. M.; "Tests and Combinations of Satellite Determinations of the Gravity Field with Gravimetry"; JGR, Volume 71, No. 22, pg. 5303; 1966.

12. Kaula, W. M.; "The Appropriate Representation of the Gravity Field for Satellite Geodesy"; Proc. IV Symposium on Math. Geodesy., Trieste; 1969.

13. Rapp, R. H.; "Geopotential Coefficient Behavior to Degree 2001"; Unpublished Draft; 18 April 1972.

14. Rapp, R. H., "Geoid Information by Wavelength", Ohio State Univ., Dept. of Geodetic Science Report. To be published.

15. Jordan, S. J., "Self Consistent Statistical Models for the Gravity Anomaly, Vertical Deflections, and Undulation of the Geoid"; JGR, Vol. 77, No. 20, pg. 3660; July 1972.

16. Blackman, R. B. and Tukey, J. W., "The Measurement of Power Spectra"; New York: Dover Publications; 1959.

17. Bendat and Piersol, "Measurement and Analysis of Random Data"; Wiley, 1966.

18. Brown, R. D. and Fury, R. J., "Determination of the Geoid from Satellite Altimeter Data - Summary of Activities"; Computer Sciences Corporation Report 5035-21000-01TM; Contract NAS5-11790; April 1972.